Hybrid waveguides for optically pumped amplifiers

S. Saini,[a] C.-Y. Hong, S. Bernardis, N. Pfaff, L. C. Kimerling, and J. Michel
Department of Materials Science and Engineering, Massachusetts Institute of Technology, Cambridge, Massachusetts 02139, USA

(Received 19 August 2008; accepted 11 February 2009; published online 6 March 2009)

A hybrid waveguide based on simultaneous propagation of photonic crystal (PC) and total internal reflection confined optical modes is introduced for a scheme to uniformly pump waveguide optical amplifiers (WOAs). Planar one-dimensional PC structures were deposited by plasma enhanced chemical vapor deposition and characterized by reflectivity as a function of angle, confirming the existence of PC defect states. Two design trade-offs, angular acceptance and critical coupling, are modeled to demonstrate optimization of optically pumped gain within the PC defect state. The advantage of uniform pumping on the WOA gain profile is briefly discussed. © *2009 American Institute of Physics*. [DOI: 10.1063/1.3094752]

Photonic crystal (PC) waveguides guide light within a "defect" region, a volume of material that disrupts the periodic refractive index profile of a composite medium in one, two, or three dimensions.[1–3] Defect regions are designed by the choice of refractive index and dimensions in order to confine wavelengths of light otherwise inhibited by the optical band gap[4] of the periodic medium. For one-dimensional (1D) PCs, light propagation occurs along the two dimensions of translational invariance, dubbed the *defect layer*.[5]

In experimental PC waveguides,[6–11] the finite amount of periodic media surrounding a defect region results in a complex propagation wavevector and thus loss in guided optical power per unit length.[6,10] The preponderance of PC waveguide applications largely focus on the reduction in this loss propagation.

In this letter we design and characterize 1D PC waveguides that employ the properties of *finite confinement*—the existence of a non-negligible propagation loss—to achieve a scheme for out-of-plane amplification[12] of optically pumped waveguide optical amplifiers (WOAs).[13] This scheme employs the hybrid PC waveguide design,[14–17] simultaneously confining and guiding light by total internal reflection (TIR) and the photonic band gap effect.

Two test structures for evaluating the proposed device were grown by plasma enhanced chemical vapor deposition (PECVD) on oxidized silicon (Si) in a Si complementary metal-oxide semiconductor-compliant cleanroom. Reflectivity measurements were done using a Carey 5E UV-vis-near infrared dual-beam spectrophotometer. Film thickness and refractive index of the individual layers were calibrated by a KLA-Tencor-Prometrix UV-1280 ellipsometer ($\lambda = 633$ nm). Theoretical reflectivity plots were calculated by means of the transfer matrix method.

Test structures 1 and 2 comprise defect layers clad by a symmetric number of periodic thin films; both structures are

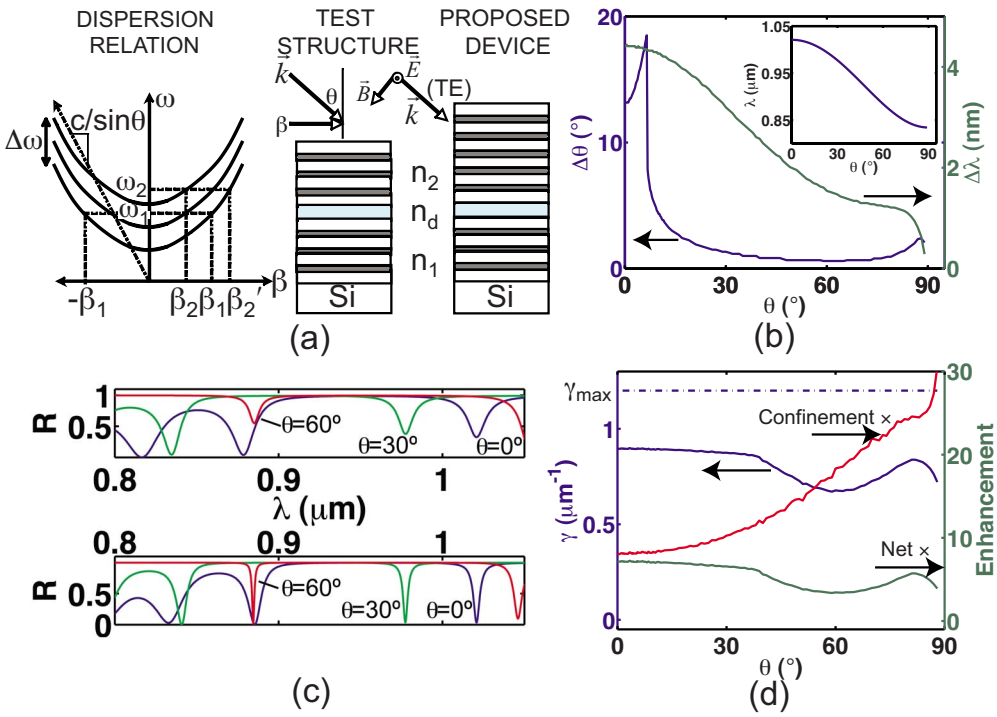

FIG. 1. (Color online) (a) Schematic diagrams. Dispersion relation depicts the uncertainty in the band structure of defect states for a finite PC with resonant transmission linewidth $\Delta\omega$. Test structure depicts orientation of light (wavevector $\vec{k}$), θ, and β with respect to deposited samples (Si substrate). Proposed device depicts orientation of TE mode light ($\vec{E}$ electric field, $\vec{B}$ magnetic field) with respect to asymmetric-clad device. (b) Angular acceptance $\Delta\theta$ and cold cavity linewidth $\Delta\lambda$ vs θ. Inset: resonant transmission wavelength λ vs θ. (c) Reflectivity R vs λ for symmetric test structure 2 (top) and asymmetric proposed device (bottom). (d) Gain γ and enhancement factors (Confinement ×, Net ×) vs θ for proposed device. γ_{max} is the upper limit due to complete population inversion of Er.

[a]Electronic mail: sajan.saini@qc.cuny.edu. Present address: Department of Physics, Queens College of CUNY, Flushing, NY 11367, USA.

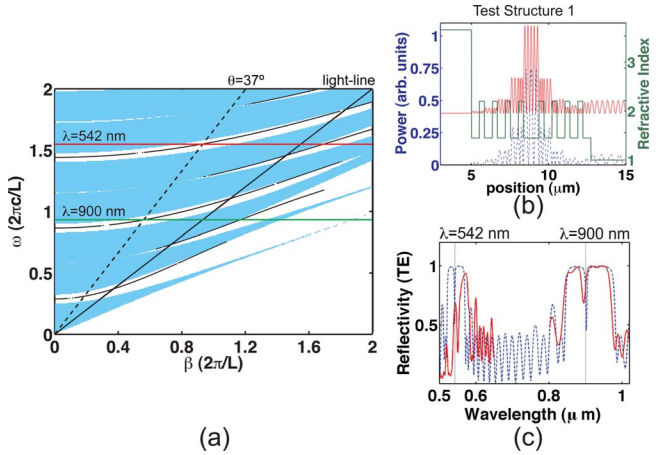

FIG. 2. (Color online) Test structure 1. (a) TE polarization photonic band diagram for the SiO_2/SiN_x 1D PC containing a SiO_2 defect layer. (b) Refractive index and power profile of confined modes at $\lambda=900$ nm (blue dashed lines) and $\lambda=542$ nm (red solid lines). (c) TE reflectivity theory (blue dashed lines) and experimental data (red solid lines) at $\theta=37°$.

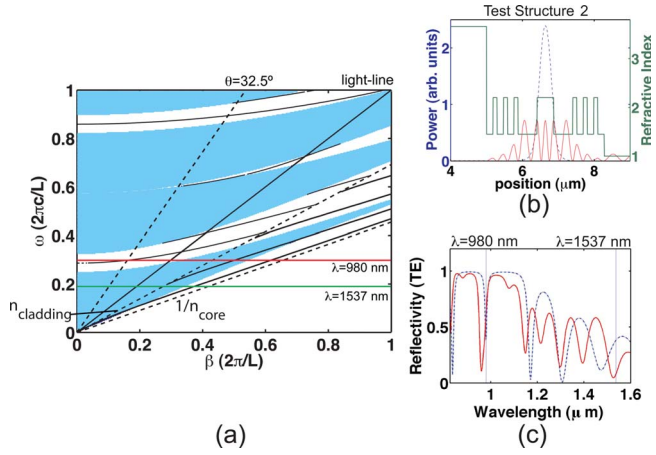

FIG. 3. (Color online) Test structure 2. (a) TE polarization photonic band diagram for the SiO_2/SiN_x 1D PC containing a SiN_x defect layer. (b) Refractive index and power profile of confined modes at $\lambda=1537$ nm (blue dashed lines) and $\lambda=980$ nm (red solid lines). (c) TE reflectivity theory (blue dashed lines) and experimental data (red solid lines) at $\theta=32.5°$.

deposited on a Si substrate [see "Test Structure" schematic in Fig. 1(a)]. Test structure 1 is a conventional PC waveguide with a silicon oxide defect layer (SiO_2; refractive index of $n_d=1.45$, film thickness of $d_d=1015$ nm), clad by periodic layers of SiO_2 ($n_1=1.45$, $d_1=515$ nm) and Si-rich silicon nitride (Si-rich Si_3N_4, i.e., SiN_x; $n_2=2.2$, $d_2=325$ nm) [see Fig. 2(b) for refractive index profile]. Figure 2(a) shows the associated 1D photonic projection band diagram for transverse electric (TE) polarization, where angular frequency of light ω and propagation constant β have been plotted in units renormalized to $2\pi c/L$ and $2\pi/L$, respectively (c is the free space speed of light and $L=d_1+d_2=839$ nm). A dispersion curve, lying within the photonic band gap (unshaded region), represents guided modes of light.

TE light of wavelength λ (wavevector $k=2\pi/\lambda$), incident from above (i.e., out-of-plane) at an angle θ with respect to the normal [see Fig. 1(a)], has $\beta=k\sin\theta$. In Fig. 2(a), wavelengths of light incident at angle θ are depicted by a line with slope $[\omega/(2\pi c/L)]/[\beta/(2\pi/L)]=1/\sin\theta$ (renormalized units). TE reflectivity at $\theta=37°$ was experimentally measured [Fig. 2(c)], demonstrating direct correspondence between (A) reflectivity stopband and the photonic band gap and (B) reflectivity resonant transmission and the dispersion curve. Figure 2(c) experimentally confirms resonant transmission close to $\lambda=542$ and 900 nm, as predicted along the $\theta=37°$ line in Fig. 2(a) (see comment two paragraphs below about fitting error). Figure 2(b) plots the modal solution for these wavelengths and confirms power confinement to within the defect layer.

The scheme proposed for out-of-plane amplification of optically pumped WOAs relies on correspondence property (B). Figure 3(b) shows the refractive index profile for test structure 2 ($n_1=1.45$, $d_1=176$ nm; $n_2=2.2$, $d_2=116$ nm). By selecting a SiN_x defect layer ($n_d=2.2$, $d_d=464$ nm) and cladding it with a thick spacer layer of SiO_2 ($d_{spacer}=540$ nm), TIR modes can simultaneously be guided within the defect layer. If the defect layer is doped with erbium (Er), these optically active centers can be pumped out-of-plane [see "Proposed Device" schematic in Fig. 1(a)] by resonant coupling of pump wavelength $\lambda_{pump}=980$ nm, while a TIR mode propagates in-plane and acquires optical gain (at $\lambda_{signal}=1537$ nm) from the population-inverted Er.

Figure 3(a) shows the photonic projection band diagram for test structure 2: at $\lambda_{pump}=980$ nm, a PC propagating mode exists above the free space light-line. At $\lambda_{signal}=1537$ nm, only a TIR propagating mode exists; this mode lies below the free space light-line and is confined within a pair of light-lines with slopes renormalized to waveguide core and cladding refractive indices. For this hybridized design, the SiN_x defect layer corresponds to a waveguide core ($n_{core}=2.2$), and the SiO_2 spacer layers correspond to waveguide cladding ($n_{cladding}=1.45$). The SiO_2 spacer layers are chosen to be $\sim 3\times d_1$, adequately isolating the TIR mode evanescent tail from the PC cladding. Figure 3(b) plots the modal solution for λ_{pump} and λ_{signal}, confirming power confinement to within the defect layer. Figure 3(c) shows experimental TE reflectivity at $\theta=32.5°$, confirming resonant transmission at $\lambda=980$ nm. For $\lambda=1537$ nm, reflectivity data do not show any stopband or resonant transmission; since the TIR waveguide propagating state lies below the free space light-line, it cannot be accessed from an out-of-plane reflectivity experiment. Transmission electron microscopy images of like-deposited samples[18] have shown a deviation in nominal layer thicknesses of 10–15 nm to account for the ± 5 nm discrepancy in resonant wavelength between experiment and theory [as seen in Figs. 2(c) and 3(c)]. We similarly attribute the presence of secondary reflectivity dips, in the experimental stopband and adjacent peaks, to these calibration deviations in PECVD deposition versus nominal design.

We conclude with two comments concerning device optimization. (1) The finite number of PC pairs implies a resonance transmission linewidth $\Delta\lambda$ or $\Delta\nu$ such that $\lambda/\Delta\lambda=\nu/\Delta\nu\simeq Q$, where Q is the cavity quality factor. A one-to-one correspondence can be made between $\Delta\lambda$ and an *angular acceptance* $\Delta\theta$ for coupling λ_{pump} from out-of-plane at angle θ. The dispersion curve schematic in Fig. 1(a) shows a parabolic band for the PC propagating mode; at $\beta=0$, the linewidth $\Delta\omega\equiv 2\pi\Delta\nu$ can be modeled by sketching two additional parabolas vertically displaced $\pm\Delta\omega/2$. For resonant transmission at ω_2, the finite linewidth implies $\beta_2<\beta<\beta_2'$. The simplest approximation of assuming all three bands having identical curvature gives the relation $\beta_2'^2-\beta_2^2=\Delta\omega/(d^2\omega/d\beta^2)$. $\beta_2'^2-\beta_2^2$ has the same qualitative trend as $\Delta\theta$; we infer that increasing either Q (more periodic layers)

or $d^2\omega/d\beta^2$ (less dispersive PC propagating mode) will decrease $\Delta\theta$. In Fig. 1(b) (left axis), we calculate $\Delta\theta(\theta)$ for the proposed device (five SiO_2/SiN_x upper cladding pairs, three lower cladding pairs; $Q \simeq 230$) using theoretical reflectivity spectra. For a given θ, the linewidth (right axis) and resonant transmission wavelength (inset) are referred to as nominal values. θ is then slightly increased (decreased) until the nominal resonant wavelength no longer lies within the $3-dB$ linewidth of the blueshifted (redshifted) resonant transmission peak. $\Delta\theta$ represents this range of θ. $\Delta\theta$ decreases monotonically with θ, except for angles close to $\theta=0°$. Figure 1(a) dispersion schematic shows (for θ close to 0°) resonant transmission at ω_1 corresponds to $-\beta_1 < \beta < \beta_1$. $\beta<0$ simply means λ_{pump} can be incident at $\theta<0°$, i.e., couple to a counterpropagating PC mode. The general trend in $\Delta\theta(\theta)$ and $\Delta\lambda(\theta)$ shows that a laser pump of given linewidth will have efficient power insertion at smaller incident angles.

(2) *Critical coupling*[19] matches the rate of power insertion through the upper cladding ("upper" mirror loss α_{m1}) into a resonant cavity to the sum of the rates of power dissipation within the cavity (absorption) and power extraction through lower cladding ("lower" mirror loss α_{m2}). Critical coupling optimizes coherent buildup of cavity power and ensures 100% resonant transmission at λ_{pump}.[20] The proposed device mirror loss, calculated from normal incidence cold cavity linewidth $\Delta\lambda$ (Ref. 19) in Fig. 1(b), is $\alpha_m=\alpha_{m1}+\alpha_{m2} \simeq 2\pi n_d \Delta\lambda/\lambda^2 \simeq 0.06\ \mu m^{-1}$. In comparison, absorption by $N=2\times10^{20}$ Er/cm^{-3} at $\lambda_{pump}=980$ nm (interaction cross-section[13] $\sigma_{pump} \simeq 10^{-21}$ cm^2) is $\alpha_{abs} \simeq (N_1-N_3)\sigma_{pump} \approx N\sigma_{pump}=2\times10^{-5}\ \mu m^{-1}$ (N_1 and N_3 are the ground and second excited state populations, respectively[13]). $\alpha_{abs} \ll \alpha_m$, implying a symmetric design such as test structure 2 (three SiO_2/SiN_x pairs in upper/lower cladding) should be close to critical coupling. However, Fig. 1(c) (top) shows theoretical reflectivity at three angles; none of the resonant peaks have close to 100% transmission because the Si substrate introduces considerable asymmetry to the refractive index profile. The proposed device has an asymmetric cladding and is thus closer to critical coupling [Fig. 1(c), bottom]. Optical gain [$\gamma \simeq (N_2-N_1)\sigma_{signal}$, N_2 is the first excited state population[13]] for the proposed device is modeled in Fig. 1(d), using the Er parameters cited in Ref. 13, with an Er concentration of 2×10^{20} cm^{-3}. Figure 1(d) (right axis) plots the pump power enhancement in the defect layer as "Confinement $\times$" $=Tn_{circ}^2=(1/\tau_{ext})/(1/t_{transit})[(1/t_{transit})/(1/\tau)]^2$. $T=1-R_1=1-e^{-\alpha_{m1}d_d} \approx \alpha_{m1}d_d=v_g t_{transit}/v_g\tau_{ext}$ is the steady-state fraction of power transmitted into the cavity through the upper cladding (with R_1 reflectivity, v_g group velocity, $t_{transit}$ time for λ_{pump} to cross the cavity). $n_{circ}=d_{eff}/d_d=v_g\tau/v_g t_{transit}$ is the number of recirculation passes of superposing traveling electromagnetic waves, trapped for an effective path length d_{eff} within the cavity, until dissipation. τ is the proposed device cavity lifetime calculated from the resonant transmission linewidth using $Q=\omega\tau \approx \lambda/\Delta\lambda$. τ_{ext} is the lifetime for insertion/extraction of power through the upper cladding; it is calculated from half the linewidth of resonant transmission through a structure with five SiO_2/SiN_x pairs cladding defect and spacer layers, with no Si substrate. (Confinement $\times$ can similarly be derived from the converging sum of transmitted electric field and higher order reflections, evaluated at the center of the cavity, for the resonant wavelength condition).[20] Net $\times$ estimates the insertion loss of the externally coupled pump by weighting Confinement $\times$ with the ratios $\Delta\theta/\Delta\theta_{laser} \cdot \Delta\lambda/\Delta\lambda_{laser}$ ($\Delta\theta_{laser}=1°$ and $\Delta\lambda_{laser}=5$ nm are the presumed angular tolerance and linewidth of the laser pump, respectively). We apply the rule $\Delta\theta/\Delta\theta_{laser}=1$ for $\Delta\theta > \Delta\theta_{laser}$ and $\Delta\lambda/\Delta\lambda_{laser}=1$ for $\Delta\lambda > \Delta\lambda_{laser}$, resulting in the flat-top feature at small angles for Net $\times$. Two trade-off comments are apparent: (a) while a higher Q with critical coupling increases Confinement $\times$, a reduction in $\Delta\theta$ and $\Delta\lambda$ implies an eventual decrease in Net $\times$ and (b) for $Q \simeq 230$, Confinement $\times$ increases with θ significantly, but the strong decrease in $\Delta\theta$ and $\Delta\lambda$ implies that Net $\times$ does not favor coupling at large angles. γ is calculated [Fig. 1(d), left axis] with Net $\times$ multiplying a pump power of 3 mW (400 μm diameter beam spot) and assuming a λ_{signal} in the defect layer of incident power 1 μW. For the proposed device, we observe that $Q \simeq 230$ provides a large enough Confinement $\times$ to invert the 2×10^{20} cm^{-3} Er population and result in $\gamma>0$.

In conclusion, we have modeled, fabricated, and measured PC test structures that demonstrate the design of a hybrid waveguide for out-of-plane optically pumped WOAs. Previously,[13] we analyzed the influence of index contrast on the gain efficiency of optically pumped WOAs: the need to co- or counter-propagate a pump wavelength results in a subexponential decay of pump power along the WOA and a nonuniform gain profile,[20] making length a critical device parameter for optimizing gain. The hybrid structure presented here allows one to circumvent this constraint and achieve the more uniform gain profile characteristic of electrically injected semiconductor optical amplifiers.

The authors would like to thank Professor K. Wada (Department of Materials Engineering, The University of Tokyo) for theoretical discussions concerning PC waveguide design.

[1] E. Yablonovitch, J. Mod. Opt. **41**, 173 (1994).
[2] J. D. Joannopoulos, P. R. Villeneuve, and S. Fan, Nature (London) **386**, 143 (1997).
[3] J. D. Joannopoulos, R. D. Meade, and J. N. Winn, *Photonic Crystals: Molding the Flow of Light* (Princeton University Press, Princeton, 1995).
[4] E. Yablonovitch, J. Opt. Soc. Am. B **10**, 283 (1993).
[5] E. Yablonovitch, T. J. Gmitter, R. D. Meade, A. M. Rappe, K. D. Brommer, and J. D. Joannopoulos, Phys. Rev. Lett. **67**, 3380 (1991).
[6] M. Ibanescu, Y. Fink, S. Fan, E. L. Thomas, and J. D. Joannopoulos, Science **289**, 415 (2000).
[7] P. Russell, Science **299**, 358 (2003).
[8] J. C. Knight, J. Opt. Soc. Am. B **24**, 1661 (2007).
[9] K. K. Lee, A. Farjadpour, Y. Avniel, J. D. Joannopoulos, and S. G. Johnson, Proc. SPIE **6901**, 69010K (2008).
[10] Y. Yi, S. Akiyama, P. Bermel, X. Duan, and L. C. Kimerling, IEEE J. Sel. Top. Quantum Electron. **12**, 1345 (2006).
[11] Y. Fink, J. N. Winn, S. Fan, J. Michel, C. Chen, J. D. Joannopoulos, and E. L. Thomas, Science **282**, 1679 (1998).
[12] M. Lipson and L. C. Kimerling, U.S. Patent No. 6,567,209 (20 May 2003).
[13] S. Saini, J. Michel, and L. C. Kimerling, J. Lightwave Technol. **21**, 2368 (2003).
[14] G. P. Nordin, S. Kim, J. Cai, and J. Jiang, Opt. Express **10**, 1334 (2002).
[15] S.A. Cerqueira, Jr., F. Luan, C. M. B. Cordeiro, A. K. George, and J. C. Knight, Opt. Express **14**, 926 (2006).
[16] L. Xiao, W. Jin, and M. S. Demokan, Opt. Express **15**, 15637 (2007).
[17] X. Sun, Opt. Lett. **32**, 2484 (2007).
[18] S. Saini, C.-Y. Hong, N. Pfaff, L. C. Kimerling, and J. Michel, Appl. Phys. Lett. **93**, 261102 (2008).
[19] H. A. Haus, *Wave and Fields in Optoelectronics* (Prentice-Hall, Saddlebrook, NJ, 1983).
[20] L. A. Coldren and S. W. Corzine, *Diode Lasers and Photonic Integrated Circuits* (Wiley, New York, 1995).